INVERSE IDENTIFICATION OF MESO-LEVEL MATERIAL PROPERTIES IN WOVEN FABRICS USING A MULTI-OBJECTIVE OPTIMIZATION TECHNIQUE

M. Komeili, A.S. Milani*

School of Engineering, University of British Columbia, Kelowna, Canada
**abbas.milani@ubc.ca*

Keywords: woven fabrics, meso-level unit cell, finite element method, multi-objective optimization, inverse identification.

Abstract

Numerical modeling of dry woven fabrics at meso level has become a powerful tool for gaining more insight into the multi-scale behavior of these materials. However, finding correct material properties for meso-level yarns is still a challenge. The current practice is to use inverse identification techniques in individual deformation modes via robust optimization procedures. Nonetheless, the problem of entrapment of numerical procedures into local minima, on one hand, and the inconsistency of final nominal sets of yarn parameters under different deformation modes, on the other hand, are among questions that need to be addressed. The inverse identification case study employed in this work on a glass plain weave is intended to demonstrate the above need. Subsequently, a multi-objective inverse identification scheme is recommended.

1 Introduction

1.1 Woven fabrics in meso level

Woven fabric composites have attracted considerable attention in the past few decades. This is not only due to the common advantage of composites such as superior mechanical performance, but also because of their ease of formability [1]. Woven fabrics are fabricated by interlacing fibrous yarns in 2D patterns. Depending on the interlacing pattern, different types of fabrics can be produced [2] (e.g., plain, twill, satin weave, etc.). The fact that fabrics are made of yarns consists of bundles of fibers indicate the multi-scale nature of these materials. Subsequently, woven fabrics have been studied in three different material levels (length scales) known as micro, meso, and macro level/scale. Each level has different representative elements and characteristic lengths [3]. Micro-level is characterized by fibers in a μm length scale. Yarns made of hundreds/thousands fibers are the representative elements of the meso-level material system, with the length scale being in the order of mm. Finally, interlaced and interwoven yarns constitute the macro-level fabric with a length scale of m/cm. In reality, woven fabrics are heterogeneous media, but due to the complexity of analytical/numerical simulations, in each level the material representative element is often assumed to be homogeneous. Nevertheless, to characterize a fabric behavior accurately, a link between different material levels is needed which is often done via homogenization techniques [4].

Studying meso-level behavior of fabrics can be useful for a robust design of composite products at macro-level [5]. Meso-level modeling provides designers with more insight towards phenomena such as stress distribution and damage initiation in the yarns during deformation [3], permeability of fabrics during resin transfer molding [6] and other similar phenomena that cannot be addressed in a merely macro-level simulation. However, the problem of finding the yarn constitutive material properties at the meso level is one of the major challenges. Two most prevailed techniques that are widely used for meso-level simulations of fabrics include the application of homogenized material properties from micro-level unit cells [4], and the use of specific hypo-elastic material behaviors based on fibrous nature of yarns [7]. The former is essentially developed for impregnated yarns, and the latter has proven to be more suitable for dry fabrics where there is no material occupying the gaps between fibers in the yarn [8]. For a dry yarn, in turn, defining a material constitutive model requires determining the model's parameters via experimental data. Due to the changes in shape, contraction and damage of yarns during weaving, it is not recommended to extract these parameters from a single yarn [9]. Moreover, removing single yarns from a fabric and running tests on them has the drawback of neglecting the effect from interactions between yarns in the woven form. Alternatively, an inverse identification technique can be a powerful tool for extracting the *effective* material properties of fibrous yarns from experimental data collected on the macro-level fabrics.

Although there have been notable efforts in the characterization of yarns using inverse identification techniques [8–10], two main gaps remain unaddressed. First, the identifications are normally pursued under a single mode of deformation (i.e., axial tension or trellis shear). Generally, woven fabrics may not be under the effect of a single deformation mode in real forming applications. Some recent studies emphasized on the existence of interactions between individual deformation modes in fabric forming and structural response [11], [12]. Second, only one set of nominal material parameters is obtained for each individual study, without any argument on the sensitivity and possible inconsistency of parameters within and between deformation modes. A recent study by Komeili and Milani [13] highlighted the effect of potential meso-level material uncertainties on the sensitivity of response of woven fabrics in each mode. The main goal of the present article, using an illustrative example on a glass plain weave, is to demonstrate the potential application of a multi-objective inverse identification methodology that may be suitable for finding material properties of yarns under general loading conditions (combined shear and tension). This includes implementing macro-level tests in different mode along with a multi-objective optimization technique.

2 Case study: Inverse identification process

2.1 Experiments

The primary input required for an inverse identification process is the reaction force (stress) vs. displacement (strain) data collected from experimental measurements on a fabric sample. For this purpose, three sets of experiments including uni-axial, bi-axial and shear frame tests were ran on a fabric sample cut from an identical role. The fabric is made of E-Glass fibrous yarns that are interlaced with a balanced plain weave pattern. The basic unit cell for the fabric and its nominal dimensions are depicted in Figure 1, where S=5.14 mm, w=4.22 mm and h=0.25 mm. Measured data points under the above tests can also be seen in Figure 2.

2.2 Meso-level numerical simulation

The meso-level unit cell for the selected woven fabric was generated using TexGen [14]. The yarn material constitutive behavior is based on the models developed in [7], which were further adapted to run with implicit integrator of the Abaqus finite element package as described by Komeili and Milani [15], [16]. The material tangential stiffness in a frame along fibers in the yarn is given by:

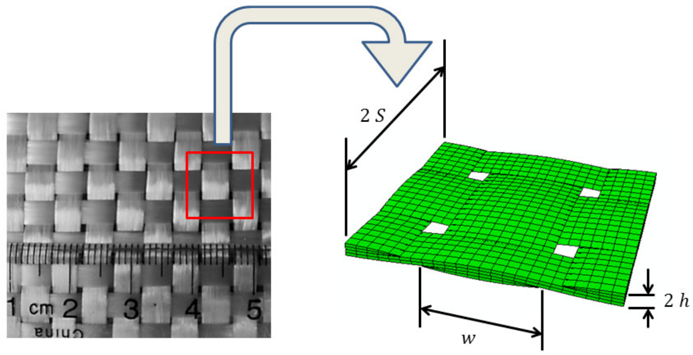

Figure 1: (a) The selected plain woven fabric; (b) fabric unit cell

$$C_f = \begin{bmatrix} E_{11} & & & & & \\ & E_{22} & & & 0 & \\ & & E_{33} & & & \\ & & & 2G_{12} & & \\ & 0 & & & 2G_{13} & \\ & & & & & 2G_{23} \end{bmatrix} \tag{1}$$

where E_{11} is the axial stiffness that is one of the parameters to be determined via inverse identification. It should be mentioned that the magnitude of E_{11} is very large for the axial tension while it is very low/negligible in compression, due to the buckling of extremely thin fibers. For the stability of numerical simulations (i.e., for imposing a nonzero stiffness state), the following relation was used between the compressive and tensile longitudinal stiffness of yarns:

$$\left(E_{11}\right)_{compression} = \frac{\left(E_{11}\right)_{tension}}{20} \tag{2}$$

In addition, the following formula was implemented for estimating the lateral yarn stiffness:

$$E_{ii} = A_0\, e^{-p\,\varepsilon_s} + E_\infty \left|\varepsilon_{11}\, \varepsilon_{ii}\right| + 5.0\,\text{MPa} \tag{3}$$

where A_0, p and E_∞ are to be determined from inverse identification, and $\varepsilon_s = \left(\varepsilon_{22} + \varepsilon_{33}\right)/2$ is the spherical strain in the transverse plane of the yarn. Equation (3) was driven from previously suggested models for crushing of dry yarns under axial tension [10] and pure shear [8]. The shear stiffness is suggested to take the form of:

$$G_{ij} = 10.0\left(1 + \left|\varepsilon_{11}\right| \times 10^3\right)\text{MPa} \tag{4}$$

A hypo-elastic constitutive behavior [7] was implemented into the code using a user-defined Fortran subroutine (UMAT). Numerical simulations were controlled with predefined displacement on four coroner points of the unit cell along with the necessary periodic boundary conditions applied on the peripheral surfaces and edges of the cell [17].

2.3 Multi-objective optimization

The task of the inverse identification is to match the predictions by numerical simulations with the data from experiments. This is done by varying the values of material parameters (E_{11}, A_0, p and E_∞) as optimization variables. To arrive at a quantitative measure of how close the simulation results are to the experimental measurements, an objective function may be defined as follows:

$$e = \sum_{i=1}^{n} \left| F_i^{sim} - F_i^{exp} \right| \Delta x_i \tag{5}$$

In which n is the number of points. F_i^{sim} and F_i^{exp} are the reaction forces in an identical state of deformation in the simulation and experimental curves, respectively; Δx_i is the strain difference in the axial modes (or shear angle in the shear mode) between two subsequent measurements (e.g., F_i and F_{i-1}). In essence, the above formula shows an approximation of the area difference between the experimental and simulation curves. Ideally, the value of the error function should be zero for a perfect model, however, in a real case it is not possible to attain this goal and thus, minimizing the error function (e) is considered to be the best solution. Moreover, for each different loading mode there may be one relevant objective function. Thus, in this case the problem turns into a multi-objective optimization. In order to express the ensuing problem more explicitly, a total objective function can be defined to convert the multi-objective optimization into a single objective optimization as follows.

$$e_{total} = \sum_{j \in modes} \frac{w_j e_j}{\alpha_j} \tag{6}$$

In Eq. (6), *modes* = {*uni-axial*, *bi-axial*, *shear*} are the three different loading modes that are studied in this case study; w_j and α_j are, respectively, the weighting factors and the scale factors used to put a relative emphasis on each mode (in case there is more importance of one mode over the others for a particular application) and to bring the scale of runs from different modes to the same level (in case the individual error functions have different magnitude orders). e_j is the individual error function that is calculated from Eq. (5) for each mode.

3 Results

Having the data from experimental measurements (Section 2.1) and the parametric numerical model (Section 2.2), an iterative optimization algorithm can be employed to conduct the inverse identification via Eq. (5) or (6). The optimization problems were solved in Isight [18] using a downhill simplex method.

3.1 Inverse identification on individual modes

Downhill simplex method is a geometrically intuitive algorithm that can be used for structural optimization problems [18]. One of the main advantages of this method is that it is not gradient-based. Moreover, because of the low number of iterations that are needed to attain convergence, compared to other exploratory and stochastic techniques, the downhill simplex method is known to be suitable for optimization problem with high computational costs. Table 1 shows the results of inverse identification via Eq. (5) for each individual deformation modes along with the corresponding objective function value. As mentioned earlier, the objective function is as an estimation of the area difference between the experimental and simulation curves. Figure 2 also shows the response curves via optimum sets of material properties in Table 1.

Model parameters	Individual deformation modes			Multi-objective case
	Uni-axial	**Bi-axial**	**Shear frame**	
E_{11} (GPa)	9.17	13.06	4.73	10.41
A_0 (kPa)	1.14	0.83	0.25	0.994
p	19.94	27.56	25.26	26.69
E_∞ (GPa)	10.64	20.76	18.20	24.43
Objective function	1.14E-4	1.05E-4	0.686	0.214

Table 1. The outcome of inverse identification for each individual mode

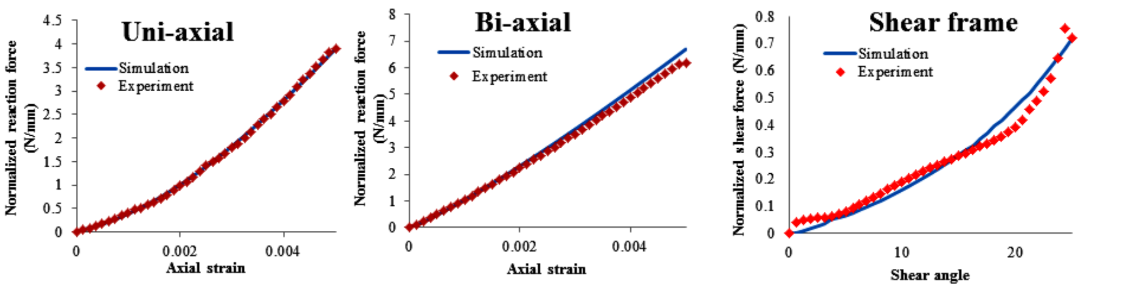

Figure 2. Comparison of experimental measurements to the simulations using material properties obtained from single inverse identification on individual modes

Although the quality of numerical predictions in each mode in Figure 2 may be acceptable, the parameters obtained for individual modes are quite different from each other as seen in Table 1; whereas ideally a given constitutive material model should posses a unique set of parameters for all deformation modes. Thus, the need for a multi-objective optimization rises for attaining meso-level yarn material parameters that can be applied to general purpose finite element simulations.

3.2 Multi-objective inverse identification

The multi-objective error function for simultaneously running inverse identification on all the three modes was defined in Eq. (6). The weighting factors for the modes are defined to be identical (the unity), in order to give them the same level of importance. For the scale factors, the estimated values of areas under the experimental curves were used. Table 1 includes the results for the multi-objective inverse identification, and the comparison of experimental and simulation data can be found in Figure 3.

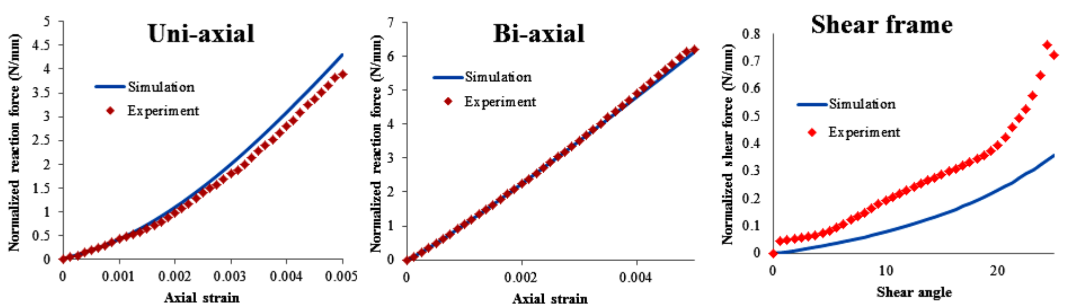

Figure 3. Comparison of experimental measurements to the simulations using data obtained from a multi-objective inverse identification on all three deformation modes

According to Figure 3, using the multi-objective optimization has led to a higher relative deviation from experimental points in each mode. Although the predictions are in the acceptable range for the tensional modes (uni-axial and bi-axial), the deviation in the shear mode has become substantial. Nonetheless, shear frame test has been proven to be a test that is highly sensitive to experimental conditions (e.g., clamps pressure) and noise sources such as fiber misalignment [1]. Some studies on handling uncertainties associated with such tests were suggested by Milani et al. [19] and can be further extended for multi-objective identification cases.

4 Summary and conclusions

Meso-level simulation of dry woven fabrics has been proved to be a powerful tool for predicting their behavior in macro scale as well as studying the local deformation mechanisms in yarns. However, finding the yarn material parameters for the meso-level is a challenging task, due to changes in yarns geometry and contraction during weaving as well as interaction of yarns during deformation. Inverse identification techniques have been widely used for this purpose under single deformation modes (e.g., axial tension or trellising shear). Nonetheless, for establishing a general purpose meso-level model that is capable of simulating fabric deformation under combined loading conditions, the effect from different modes should be studied at the same time.

In this work, a general inverse identification scheme using experimental data collected from three different deformation modes (uni-axial and bi-axial tension, and trellising shear) on the same fabric (glass plain weave) was considered. Optimization using the down-hill simplex method was utilized for minimizing the deviation of simulations from experimental measurements. First, an inverse identification was conducted on each individual deformation mode and the optimum material constants were extracted. Although the simulation curves and experimental measurements showed agreeable correspondence, there are notable differences in the values of material constants obtained for each mode. Therefore, multi-objective optimization has been suggested to obtain one single set of material parameters for all modes. Results of the multi-objective inverse identification showed that although the deviation of experimental results from simulation is higher in this case, they are still within an acceptable range under axial modes. For improving the outcome of the methodology, more exploration on the effect of noise in the experiments, especially for the shear mode, and including different weighting factors may be worthwhile for the next step of this research.

Acknowledgement

The authors would like to acknowledge financial support from the Natural Sciences and Engineering Research Council (NSERC) of Canada.

References

[1] Cao J., Akkerman R., Boisse P., Chen J., Cheng H., Degraaf E., Gorczyca J., Harrison P., Hivet G., Launay J. Characterization of mechanical behavior of woven fabrics: Experimental methods and benchmark results. *Composites Part A: Applied Science and Manufacturing*, **39**, 6, pp. 1037-1053 (2008).

[2] Ishikawa T., Chou T.W. Stiffness and strength behaviour of woven fabric composites, *Journal of Materials Science*, **17**, 11, pp. 3211–3220 (1982).

[3] Lomov, S., Ivanov D., Verpoest I., Zako M., Kurashiki T., Nakai H., Hirosawa S. Meso-FE modelling of textile composites: Road map, data flow and algorithms. *Composites Science and Technology*, **67**, 9, pp. 1870-1891 (2007).

[4] Peng X., Cao J. A dual homogenization and finite element approach for material characterization of textile composites. *Composites Part B*, **33**, 1, pp. 45–56 (2002).

[5] Guagliano M., Riva E. Mechanical behaviour prediction in plain weave composites. *Journal of strain analysis for engineering design*, **36**, 2, pp. 153-162 (2001).

[6] Verpoest I., Lomov S., Virtual textile composites software□: Integration with micro-mechanical, permeability and structural analysis. *Composites Science and Technology*, **65**, 15–16, pp. 2563-2574 (2005).

[7] Badel P., Vidal-Salle E., Boisse P. Large deformation analysis of fibrous materials using rate constitutive equations. *Computers & Structures*, **86**, 11–12, pp. 1164-1175 (2008).

[8] Badel P., Vidal-Salle E., Maire E., Boisse P. Simulation and tomography analysis of textile composite reinforcement deformation at the mesoscopic scale. *Composites Science and Technology*, **68**, 12, pp. 2433-2440 (2008).

[9] Charmetant A., Vidal-Sallé E., Boisse P. Hyperelastic modelling for mesoscopic analyses of composite reinforcements. *Composites Science and Technology*, **71**, 14, 1623-1631 (2011).

[10] Gasser A., Boisse P., Hanklar S. Mechanical behaviour of dry fabric reinforcements. 3D simulations versus biaxial tests. *Computational Materials Science*, **17**, 1, pp. 7–20 (2000).

[11] Cavallaro P.V., Sadegh A.M., Quigley C.J., Johnson A.R. Effects of Coupled Biaxial Tension and Shear Stresses on Decrimping Behavior in Pressurized Woven Fabrics. *Techinal report: Naval Undersea Warfare Center* (2004).

[12] Launay J., Hivet G., Duong A., Boisse P. Experimental analysis of the influence of tensions on in plane shear behaviour of woven composite reinforcements. *Composites Science and Technology*, 68, 2, pp. 506-515, (2008).

[13] Komeili M., Milani A.S. *Meso-Level Analysis of Uncertainties in Woven Fabrics*. VDM Verlag Dr. Muller GmbH & C. KG (2010).

[14] Sherburn M. Geometric and Mechanical Modelling of Textiles. *PhD thesis University of Nottingham* (2007)

[15] Komeili M., Milani A.S. The effect of meso-level uncertainties on the mechanical response of woven fabric composites under axial loading. *Computers & Structures*, **90-91**, pp. 163-171 (2011).

[16] Komeili M., Milani A.S. *A comparison of implicit and explicit finite element methods for the meso-level simulation of dry woven fabric composites* in Proceeding of *18th International conference on composite materials*, Jeju island, Korea, (2011).

[17] Badel P., Vidal-Salle E., Boisse P. Computational determination of in-plane shear mechanical behaviour of textile composite reinforcements. *Computational Materials Science*, **40**, 4, pp. 439-448 (2007).

[18] SIMULIA, "Isight 5.5." Dassault Systèmes, 2011.

[19] Milani A.S., Nemes J., Abeyaratne R., Holzapfel G., A method for the approximation of non-uniform fiber misalignment in textile composites using picture frame test. *Composites Part A: Applied Science and Manufacturing*, **38**, 6, pp. 1493-1501 (2007).